Microchemical Journal 193 (2023) 109183

Contents lists available at ScienceDirect

Microchemical Journal

journal homepage: www.elsevier.com/locate/microc

Valorization of citrus waste for circular economy: A case study on bergamot pomace as sorbent for Cd^{2+} removal and source of added value compounds

Anna Irto [a], Salvatore Giovanni Michele Raccuia [a], Gabriele Lando [a,*], Concetta De Stefano [a], Katia Arena [a], Tania Maria Grazia Salerno [a,*], Alberto Pettignano [b], Francesco Cacciola [c], Luigi Mondello [a,d,e], Paola Cardiano [a]

[a] Department of Chemical, Biological, Pharmaceutical, and Environmental Sciences, University of Messina, 98168 Messina, Italy
[b] Department of Physics and Chemistry – Emilio Segrè, University of Palermo, I-90128 Palermo, Italy
[c] Department of Biomedical, Dental, Morphological and Functional Imaging Sciences, University of Messina, 98125 Messina, Italy
[d] Chromaleont S.r.l., c/o Department of Chemical, Biological, Pharmaceutical, and Environmental Sciences, University of Messina, 98168 Messina, Italy
[e] Department of Sciences and Technologies for Human and Environment, University Campus Bio-Medico of Rome, 00128 Rome, Italy

ARTICLE INFO

Keywords:
Waste recycling
Cadmium
Sorption/desorption
Chemical speciation
Isotherm
Flavonoids

ABSTRACT

The potential of bergamot pomace for the development of materials able to efficiently remove cadmium(II) from water and for the recovery of bioactive compounds has been explored. To this purpose, raw bergamot waste resulting after industrial essential oil and juice extraction was mechanically ground, desiccated, pretreated with various chemicals (e.g. NaOH, HNO_3, H_2O_2, H_2O, 2-propanol) and dried up to constant weight thus affording solid samples that were characterized by ATR FT-IR spectroscopy. The solutions recovered after the pomace pretreatments were investigated by means of HPLC in combination with PDA and MS detectors to assess the residual content of bioactive components, e.g., phenolic and oxygenated heterocyclic compounds (OHCs). Potentiometric studies were performed on suspensions at $t = 25$ °C, $I = 0.10$ mol dm^{-3} in $NaNO_{3(aq)}$ to investigate pomace acid-base properties and binding ability towards Cd^{2+} ions. Sorption efficiency was investigated by means of kinetic and isotherm batch experiments and resulted to be 92 ± 7 mg g^{-1}. Once loaded, sorbent reusability was tested by performing metal stripping cycles using various desorbents (HCl, HNO_3, L-GLDA, S,S-EDDS, EDTA) with an efficiency of ~ 60% after one cycle. The equilibrium Cd^{2+} concentration in solution was determined by differential pulse voltammetry and ICP-OES.

1. Introduction

Citrus transformation industries generate significant amounts of by-products, including wastewater and solid residues [1]. These latter, known as pomaces, consist of peels, endocarp membranes, seeds, residues of the juice sacs, and albedo [2]. Improper handling and direct disposal of citrus waste can lead to environmental pollution, including soil and water contamination [3]. However, citrus waste can be effectively utilized for various purposes such as animal feed, compost production, soil conditioning [4], as well as processed in biorefineries sector [5]. Furthermore, these waste materials contain biologically active compounds like polyphenols, terpenes, vitamins, pectin, fibers, making them suitable for applications in industries such as cosmetics, pharmaceuticals, chemicals, and food [6].

To address the challenges associated with citrus waste management and promote sustainable practices, supranational bodies have emphasized the reduction of waste generation and the implementation of circular economy principles aiming to minimize waste and maximize resource utilization. The development of novel approaches in managing waste biomass and extracting value from citrus residues is a critical area of focus in applied research and government programs, such as the Italian "PNRR, Mission 2C1, Circular economy and sustainable agriculture". From this perspective citrus waste, for instance, has been successfully employed as a suitable platform for the development of multifunctional materials. These materials demonstrate efficient and selective interactions with both organic (such as pesticides, dyes, drugs, POPs) and inorganic (including metals and anions) contaminants, by sorption mechanisms [7]. Furthermore, citrus waste serves as a source of added value compounds [6,8,9].

Among water pollutants, Cd^{2+} has received great attention since it

* Corresponding authors.
E-mail addresses: glando@unime.it (G. Lando), taniamariagrazia.salerno@unime.it (T.M.G. Salerno).

https://doi.org/10.1016/j.microc.2023.109183
Received 30 May 2023; Received in revised form 11 July 2023; Accepted 3 August 2023
Available online 5 August 2023

has been recognized harmful for humans, even at low levels [10], and because its concentration along the food chains may increase due to biomagnification [11]. Although cadmium naturally occurs in the environment [12] due to volcanic emissions, anthropogenic activities such as Ni-Cd batteries manufacturing, incineration of municipal waste, phosphate fertilizers production, as well as electric and electronic waste recycling, greatly affect its environmental level [13]. Sorption-based strategies, specifically for water treatment, have gained attention due to their low cost and energy-saving nature [14,15]. Various waste biomass, including agri-food waste [16], have been proposed as sorbents or matrixes for functionalization due to their reliable sorption capabilities and regeneration potential [17–21]. Carbon-based sorbents derived from waste biomass [22,23] present an opportunity for circular re-use, where end-of-life goods can be recycled as feedstock.

This contribution presents the preliminary results of a wider project focused on evaluating the potential use of bergamot pomace as sorbent for Cd^{2+} sequestration and as source of value-added molecules. Bergamot, a lesser-known citrus fruit, possesses therapeutical effects [24], and is currently utilized for essential oils and juices extraction. Here, waste generated from the industrial supply chain of bergamot was subjected to mechanical grinding, drying and various chemical pretreatments (e.g. NaOH, HNO_3, H_2O_2, H_2O, 2-propanol) to enhance its metal sorption capacity [24–27].

Several studies have shown that *Citrus* by-products (peels, seeds, pulps and exhausted peals) can contain a high amount of bioactive compounds [24,28–32]. Therefore, the solutions recovered after the pretreatments were analyzed by means of HPLC in combination with PDA and MS detectors, for the characterization of phenols and oxygenated heterocyclic compounds (OHCs). In detail, the qualitative and quantitative characterization of phenols was carried out by HPLC-PDA-MS, whereas a liquid chromatography system coupled with a triple quadrupole mass spectrometer (HPLC-MS/MS) working in multiple reaction monitoring mode (MRM) and a pre-targeted analytical method specifically developed to determine *Citrus* OHCs content was used [33]. Solids samples were characterized by ATR FT-IR spectroscopy to assess surface functional groups. Acid-base properties and Cd^{2+} binding ability of the solids were studied by potentiometric titrations. Moreover, their sorption capacity was investigated by means of kinetic and isotherm batch experiments. Furthermore, metal desorption, biomass stability and potential reusability for multiple cycles were investigated by using different desorbing agents (HCl, HNO_3, L-GLDA, S,S-EDDS, EDTA) and performing in batch studies at various experimental conditions, optimized by means of a full factorial experimental design. The equilibrium concentration of Cd^{2+} in solution was determined by means of differential pulse anodic stripping voltammetry (DP-ASV) for kinetic experiments and ICP-OES techniques for batch experiments.

Among the available literature papers on the production of sorbent materials from citrus waste biomasses, none of them have explored the use of bergamot industrial by-products for circular re-use. This study aims to fill this research gap by providing a comprehensive examination of the bergamot industry waste, exploring and critically comparing the potential of solid and liquid residues resulting from the pretreatments of this understudied matrix. This work represents a significant contribution to the existing literature findings and offers valuable insights not only to chemists but also to researchers and stakeholders in related fields.

2. Materials and methods

2.1. Materials

A sample of 5 kg of bergamot pomace (seeds, pulp, and deoiled flavedo after essential oil and juice extraction) from the *Femminello* and *Fantastico* cultivars, representative of the November 2021-January 2022 harvesting season, were provided by the *Capua 1880* company (Reggio Calabria, Italy). A portion of the supplied pristine (*raw*) bergamot pomace was mechanically ground, dried in an oven at $t = 60$ °C up to constant weight and ground again to obtain a fine powder. The resulting solid (P1, *dry* pomace) was divided in six fractions (P1-a ÷ P1-f, Table S1) and pretreated using different reagents. *Dry* pomace was pretreated exploiting various procedures already reported in the literature [24–27]. In detail, a weighed amount of P1 was put in contact with deionized water at $t = 30$ °C (P1-a aliquot) and 100 °C (P1-b), sodium hydroxide (P1-c), nitric acid (P1-d), a H_2O_2 30% solution (P1-e) and a 2-propanol 10% solution (P1-f) at $t = 30$ °C. Each mixture was centrifuged at 5000 rot m^{-1} for 5 min at $t = 25$ °C to separate the solid from the liquid phases. The supernatant was removed and subsequently analysed by HPLC-PDA-MS and HPLC-MS/MS instrument (section 2.2.4.) for the characterization of phenol and OHCs, respectively. The solid residues were washed several times with deionized water and then centrifuged, up to a constant pH value (±0.05 pH units) between two subsequent washing cycles. Then, solids were dried in an oven at $t = 60$ °C up to a constant weight (average yield *ca.* 40%) and then mechanically ground to obtain a fine powder. Full details about pretreatments are reported in the Supplementary Material, Table S1-S2, Fig. S1.

2.2. Experimental methodologies

2.2.1. Potentiometric titrations

The acid-base properties of pretreated pomace samples and their complexing ability towards Cd^{2+} were investigated by means of potentiometric measurements performed employing a Metrohm (Herisau, Switzerland) 809 Titrando equipped with a 10 cm^3 automatic burette and a combined "sure flow" glass electrode (Orion 8172BNWP). Additional information on the potentiometric apparatus and the procedure are reported in literature [34–36]. Potentiometric titrations were performed on 25 cm^3 suspensions containing about 50 mg of pretreated pomace, nitric acid and sodium nitrate to reach selected pH (~2.0) and ionic strength ($I = 0.10$ mol dm^{-3}) values, respectively. In the case of titrations involving also Cd^{2+}, the metal cation was added as $Cd(NO_3)_2 \cdot 4\ H_2O$ (0.9–1.1 mmol dm^{-3}). Titrant consisted of a standard $NaOH_{(aq)}$ solution.

2.2.2. Cadmium sorption and desorption experiments

Kinetic measurements were carried out recording different voltammograms as a function of time. The procedure started with a first scan at $t = 0$ s on a 25 cm^3 aqueous solution containing HNO_3, $NaNO_3$ as background electrolyte ($I = 0.10$ mol dm^{-3}) and Cd(II) ($c_{Cd} = 0.40$ mg dm^{-3}). Then, an aliquot of about 30 mg of solid sorbent was added to the measurement cell, and one scan per minute was carried out up to "t_e", namely the time required to reach equilibrium between the solid and the solution. Kinetics was studied according to a Pseudo First Order (PFO) and a Pseudo Second Order (PSO) kinetics [37], expressed by the following integrated (eqs. 1–2):

$$Q_t = Q_e\ (1\text{-}e^{-k_1 t}) \tag{1}$$

$$Q_t = \frac{Q_e^{\,2} k_2\ t}{1 + \ Q_e k_2\ t} \tag{2}$$

where Q_t is the sorption capacity (mg g^{-1}) at time t (s), Q_e is the sorption capacity at equilibrium (mg g^{-1}), k_1 is the PFO kinetics constant (s^{-1}), k_2 is the PSO kinetics constant (dm^3 mol^{-1} s^{-1}).

Voltammograms were collected by means of a Metrohm (Herisau, Switzerland) 663 VA Stand (Series 05) workstation, equipped with a three-electrode system, featured by a Multimode Mercury Electrode working in HDME (Hanging Mercury Drop Electrode) mode, a platinum wire auxiliary electrode and a double junction Ag/AgCl/KCl (3.0 mol dm^{-3}) reference electrode. The workstation was connected to a potentiostat (μAutolab type III)/galvanostat with IME663 interface (Eco Chemie, Herisau, Switzerland). The whole system was controlled by means of GPES v. 4.9 software (Eco Chemie, Herisau, Switzerland). Purified nitrogen was bubbled into the solutions/suspensions for 300 s

before all the experiments. The working conditions were as follows: deposition potential = −0.90 V, deposition time = 10 s, equilibration time = 10 s, modulation amplitude = 25 mV.

Sorption isotherm batch experiments were carried out on P1-a ÷ P1-f samples putting different amounts of each sorbent (10–130 mg, details in Table S3) in contact with 100–150 cm^3 of Cd^{2+} solution (*ca.* 20 mg dm^{-3}). The suspensions were stirred for 24 h at 120 mot min^{-1} in a thermostated chamber at $t = 25 \pm 1$ °C. Then, they were filtered on paper and the pH values as well as metal concentration of each solution at equilibrium were measured. The estimation of the sorption capacity was assessed by the Q_e parameter (eq. (3):

$$Q_e = \frac{(C_0 - C_e)\cdot V}{m} \quad (3)$$

where C_0 and C_e are the starting and equilibrium metal concentrations (mg dm^{-3}), respectively, V is the volume (dm^3) of the cadmium(II) solution and m is the mass of sorbent (g). The obtained data were then plotted and analyzed using a modified Langmuir type equation (see below).

Prior to perform desorption studies, bergamot pomace was loaded with Cd^{2+} by contacting 600 mg of the P1-a sample with 300 cm^3 of a *ca.* 300 mg dm^{-3} cadmium(II) solution. This suspension was stirred for 24 h at 120 mot min^{-1} in a thermostated chamber at $t = 25 \pm 1$ °C, filtered, and dried in oven at $t = 60$ °C up to constant weight. The sorption capacity before stripping test (q_0) was obtained as in eq. (3). Desorption batch experiments were performed by contacting 10 mg of the loaded pomace with 20 cm^3 of aqueous solution containing the desorbing agent (HCl, HNO_3, L-GLDA, S,S-EDDS, EDTA) in different conditions of contact time, temperature and concentration, according to a full factorial experimental design [38]. Suspensions were stirred at 120 mot min^{-1} in a thermostated chamber at $t = 25$ and 45 °C (±1) and the experiments were performed at various eluent concentrations ([L] = 0.008 and 0.10 mol dm^{-3}) and contact times (tc = 30 and 60 min). The experimental matrix containing all the details is given in Supporting Material (Table S4). Then, the suspensions were filtered, and the solutions analysed to obtain the sorption capacity after stripping test (q).

The desorption efficiency *DE* (%) [39] was calculated by means of eq (4):

$$DE = \frac{(q_0 - q)}{q_0} \cdot 100 \quad (4)$$

where q_0 and q are the sorption capacities (mg g^{-1}) loaded on sorbent before and after stripping tests, respectively.

An ICP-OES Perkin Elmer (Waltham, Massachusetts, United States), Model Optima 2100, equipped with an auto sampler model AS-90 was used to determine the equilibrium Cd(II) concentration both for sorption and desorption experiments. The cadmium(II) emission intensity was measured at the wavelength 226.502 nm and each measurement was repeated three times. The quantification of Cd^{2+} was performed by building calibration curves in the metal concentration range 1.00–30.00 mg dm^{-3}.

2.2.3. ATR FT-IR

Infrared spectra were acquired on sorbent samples using a FT-IR iS50 Nicolet Thermo Scientific spectrometer equipped with ATR diamond window module, in the middle infrared range (from 4000 to 400 cm^{-1}), accumulating 32 scans, with a spectral resolution of 4 cm^{-1}. Before analyses, the samples (details are reported in Table S5) were ground using an agate mortar to obtain a powder texture.

2.2.4. Determination of phenolic and oxygenated heterocyclic compounds

The HPLC-PDA-MS analyses of phenolic compounds were performed on a Nexera Series LC-40 (Shimadzu, Duisburg, Germany) equipped with a CBM 20A controller, one LC-40B X3 dual-plunger parallel-flow pumps, a CTO-40C column oven, a SIL-40CX3 autosampler, an SPD-M40 photodiode array, and LCMS-8050 mass spectrometer equipped with ESI interface (Shimadzu, Duisburg, Germany). Phenolic compounds were separated on an Ascentis Express C18 column (150 × 4.6 mm, 2.7 μm dp Merck KGaA, Darmstadt, Germany), with 0.1 % formic acid in water (pH ~ 3; solvent A) and 0.1 % formic acid in acetonitrile (solvent B) under the following conditions: 0–40 min, 5–25 % B; 40–60 min, 25–100 % B; 60–70 min, 100 % B. The flow rate was 0.7 mL min^{-1}. The injection volume was 2 μL and the oven temperature was set at $t = 30$ °C. The PDA parameters were performed in the wavelength range 190–400 nm, sampling frequency 40 Hz, time constant 0.025 s. The chromatograms were extracted at 210, 283 and 325 nm. The MS acquisitions were performed using ESI source operating both in positive (+) and negative ionization modes (-), with the following parameters: interface and desolvation temperature were set at 350 °C and 600 °C, respectively; heat block temperature, 300 °C; nebulizing gas flow (N_2), 1.5 L min^{-1}; drying gas flow (N_2), 15 L min^{-1}; acquisition range, 100–700 *m/z* (+/-). Data acquisition and processing was handled by the LabSolution ver. 5.95 software X2 (Shimadzu, Duisburg, Germany). Quantitative analyses were carried out using external calibration, by building calibration curves, using the area obtained in the chromatogram after triplicate injections, at five different concentration levels (1–1000 mg L^{-1}) of a mixture of six standards, namely, ferulic acid, sinapic acid, apigenin 7-O-glucoside, neodiosmin, eriocitrin, naringin as representative of the distinct chemical classes under evaluation. When the commercial standard was not available, the compounds were quantified using the calibration curve of the structurally closest related standard assuming a similar response in the PDA and having similar UV–Vis absorption maxima.

HPLC–MS/MS analyses were carried out using instrumentation consisting of a Shimadzu *Nexera* X2 UHPLC, and a triple quadrupole mass spectrometer LCMS-8060 (Shimadzu, Duisburg, Germany). An Atmospheric Pressure Chemical Ionization (APCI) interface, working in positive ionization mode was used as MS source. Analytical conditions for chromatographic separation and MS parameters have already been reported [33,40]. Briefly, separation occurred on a 50 × 4.6 mm, 2.7 μm Ascentis Express C18 column (Merck KGaA, Darmstadt, Germany). Gradient program was 0–4.5 min, 15–28 % B; 4.5–7.0 min, 28–60 % B; 7.0–11.0 min, 60–85 % B, 11.0–14.0, 85 % B. Water/methanol/THF (85/10/5, *v/v/v*) was used as mobile phase (A) and methanol/THF (95/5, *v/v*) as mobile phase (B). Oven temperature was set at 40 °C, injection volume was 2 μL. MS parameters were set as follows: Interface Temp., 450 °C; DL Temp., 300 °C; Heat Block Temp., 300 °C; Drying gas flow, 15 L min^{-1}; Heat gas flow, 3 L min^{-1}; CID gas, 270 kPa. Analysis of the Cs, FCs and PMFs, were performed using the MS triple quadrupole in MRM acquisition mode, using specific acquisition windows based on retention time of target analytes. The MRM parameters (Q, quantifier ion; q, qualifier ion; CE, collision energy; Q1 and Q3 pre-bias) were optimized by the direct injection of 2 μL of different standards mixture at concentration 10 mg L^{-1}. The optimization was performed using automatic procedures of the LabSolutions software (version 5.86 Shimadzu).

Quantitative analyses were carried out using external calibration, by building calibration curves in MRM mode for each target analyte in EtOH at concentration ranging from 0.001 mg L^{-1} to 5.00 mg L^{-1}. Limit of detection (LODs), limit of quantification (LOQs), were calculated according to Eurachem guidelines as previously reported [33].

2.3. Computer programs and equilibrium constants

BSTAC computer program [41] was used for the analysis of potentiometric titrations for refinement of reagents analytical concentrations, ionic product of water (log K_w), standard electrode potential (E^0) and liquid junction potential coefficient (j_a) [42], as well as for the determination of the equilibrium constants. The non-linear least squares LIANA (LInear And Nonlinear Analysis) program [41] was employed for fitting different equations. Speciation diagrams were drawn by means of HySS program [43], used in the case of many equilibrium studies

reported literature [44–46] for the investigation of the species distribution along the pH of analysis.

3. Results and discussion

3.1. Characterization of dry pomace

The weight loss of *raw* pristine, relative to water and other volatile compounds, resulted to be around the 85 %, in agreement with the humidity content (72.5–87.0 %) reported in literature for analogous citrus wastes [4]. As can be inferred from Fig. 1, the ATR FT-IR spectrum of the *dry* pomace (P1) displayed a profile comparable to those already reported for similar matrices such as pomelo, grapefruit and orange peels [25,47,48] and wastes [49,50], as well as for other typologies of biomasses such as algae [51], or organic matter in soil [52]. More in detail, the spectrum showed a broad band at 3313.29 cm^{-1} that can be confidently assigned to the stretching vibration of –OH groups possibly arising from pectin alcohol and carboxylic acid groups and from cellulose hydroxylic groups, present in the bergamot waste material [47], together with peaks at 2922.90 and 2851.06 cm^{-1}, due to the symmetric and asymmetric stretching of alkyl ($–CH_n$) groups [53]. Furthermore, the spectrum displayed a signal at 1719.60 cm^{-1} due to the stretching vibration of C = O bond of non-ionic (–COOH, $–COOCH_3$) carboxylic groups [54] and the typical bands of asymmetric and symmetric stretching vibrations of ionic ($–COO^-$) carboxylic groups at 1618.29 and 1406.38 cm^{-1}, respectively [50]. In addition, the peaks at 1368.74, 1047.36 and 1015.40 cm^{-1} could be attributable to the C-O stretching of carboxylic acids and alcohols [49], whereas the signal at 894.33 cm^{-1} to the C-O-C stretching from cellulose [55].

3.2. Pretreatments on dry pomace

Dry pomace was pretreated in various conditions, to ascertain which could be the most suitable approach to enhance the material sorption capability towards cadmium(II). Full experimental details about the pretreatments of *dry* pomace (P1) are given in Table S1. As expected, the *dry* pomace pretreatments led to different weight losses. In particular, the lowest loss (52 %) was observed for the P1-a aliquot. On the contrary, the highest one (64 %) was detected in the case of pretreatment with water at $t = 100$ °C for 20 min. According to literature data [27], the expected weight loss is around 50 %.

The ATR FT-IR spectra recorded on all the pretreated solids showed bands with lower intensity, although featured by similar frequencies, with respect to the ones collected for *dry* pomace. The main differences among the analysed samples were detected, in some cases, in term of relative intensity ratios between the peaks detected in the ranges 1720–1735 cm^{-1} and 1618–1640 cm^{-1} (examples in Fig. S2) due, as said, to non-ionic and ionic (asymmetric) carboxylic groups [49,50], respectively. The analysis on *dry* pomace and on the samples pretreated with H_2O (P1-a, P1-b), HNO_3 (P1-d), H_2O_2 (P1-e) and 2-propanol (P1-f), showed quite similar intensities for the two signals and, consequently, relative ratios of *ca.* 1, thus confirming findings reported in the literature for lemon and orange peel waste treated with 0.10 mol dm^{-3} HNO_3 [25,56]. On the contrary, P1-c spectrum showed a decrease of the non-ionic signal intensity at about 1734 cm^{-1}, together with an increase of the COO^- peak (1613 cm^{-1}), so that, in this case, their relative ratio reached a value of about 2. The analysis of samples obtained by carrying out two pretreatment trials using higher *dry* pomace-to-base ratios (e.g. 1:100, 1:150, pH ~ 12, Fig. S2) showed the total disappearance of the signal at 1734 cm^{-1}, thus indicating that saponification occurred, in agreement with literature data reported for lemon peel waste and modified pectin treated with NaOH at pH ~ 12 [57,58].

3.3. Acid-base properties of pomace aliquots and complexing ability towards Cd^{2+}

Potentiometric measurements on P1-a ÷ P1-f aliquots were carried out at $I = 0.10$ mol dm^{-3} in $NaNO_{3(aq)}$ and $t = 25$ °C in the pH range 2.0–11.0. The elaboration of experimental data allowed to determine the total site concentrations (meq g^{-1}) and two acidic constants assigned to functional groups named as POM_1 and POM_2. The results obtained for each aliquot and analysing simultaneously all titrations are listed in Table 1.

Considering that the sorbent is a natural product with a very complex matrix, the two acidic constants cannot be attributed to specific functional groups, and their concentration should be considered different. However, the detected values ($\log K^{H}_{POM_1} = 10.69$ and $\log K^{H}_{POM_2} = 3.50$) suggest that they could be attributed to hydroxyl (POM_1) and carboxylic (POM_2) groups. Noteworthy, both deprotonated POM_1 and POM_2 are here arbitrarily indicated as negatively charged species.

Our results can be compared only with few reliable papers present in the literature; among them, that of Schiewer et al. [59] is performed on “protonated pectin peels”, that is an acidic pretreated by-product

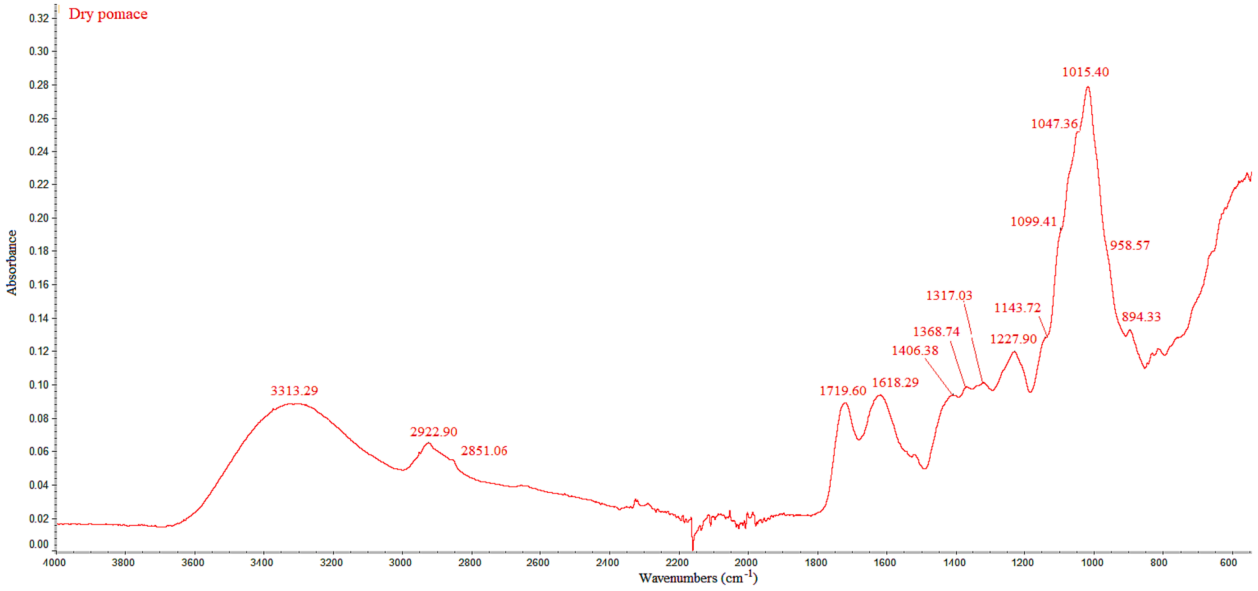

Fig. 1. ATR FT-IR spectrum of *dry* pomace (P1).

Table 1
Experimental acidic constants, total sites concentration (meq g^{-1}) of POM_1 and POM_2 determined for the different P1-a ÷ P1-f aliquots at $I = 0.10$ mol dm^{-3} in $NaNO_{3(aq)}$, $t = 25$ °C.

Aliquot	$\log K^{H}_{POM_1}$ [a]	meq g^{-1}	$\log K^{H}_{POM_2}$ [b]	meq g^{-1}
P1-a	10.55 ± 0.01[c]	1.05 ± 0.01[c]	3.56 ± 0.01[c]	1.12 ± 0.02[c]
P1-b	10.50 ± 0.01	1.03 ± 0.01	3.35 ± 0.01	1.02 ± 0.01
P1-c	11.05 ± 0.01	1.56 ± 0.03	3.55 ± 0.01	0.92 ± 0.01
P1-d	10.76 ± 0.03	1.07 ± 0.01	3.41 ± 0.01	0.90 ± 0.01
P1-e	10.49 ± 0.03	0.69 ± 0.01	3.62 ± 0.01	0.98 ± 0.01
P1-f	10.95 ± 0.06	1.27 ± 0.02	3.46 ± 0.01	1.03 ± 0.01
P1-a ÷ P1-f	10.69 ± 0.03	0.97 ± 0.02	3.50 ± 0.01	1.00 ± 0.01

[a] $H^+ + POM_1 = H(POM_1)$; [b] $H^+ + POM_2 = H(POM_2)$; [c] ± std. dev.

obtained from lemon juice manufacturing. These authors determined four acidic constants with the following values: log $K_{a1} = 3.8$, log $K_{a2} = 6.5$, log $K_{a3} = 8.4$ and log $K_{a4} = 10.7$ with the corresponding site concentrations: $B_{T1} = 0.39$, $B_{T2} = 0.11$, $B_{T3} = 0.27$, and $B_{T4} = 0.17$ meq g^{-1} together with a value of $B_{T0} = 0.2$ meq g^{-1} associated to a fairly strong acidic group (log $K_{a0} < 2$). According to the authors the four acidic constants refer to carboxylate (belonging to pectin, log K_{a1}), phosphate (log K_{a2}, log K_{a3}) and phenolic groups (log K_{a4}) [60]. However, although the acidic pretreatment on the natural product is actually the same, some important difference among the literature and this study must be remarked: i) these authors used a different citrus (lemon) than that studied in this work (bergamot); ii) mentioned results refer to "pectin peels", a by-product obtained by leaching off the water soluble sugars in the juice manufacturing, thus probably containing mostly juiced endocarp and albedo, whereas this work is performed on a pomace, a by-product obtained after both essential oil and juice extraction and then containing also deoiled flavedo. The acidic constants obtained in this work are in a very good agreement with the pK_{a1} and pK_{a4} reported by Schiewer and Patil [59], but the acidic constants related to the presence of phosphate were not determined in this work.

The site total concentration, as sum of POM_1 and POM_2, here obtained (1.97 meq g^{-1}) is significantly higher compared to the value reported by Schiewer et al. [59] (1.14 meq g^{-1} as sum of all sites) and by Reddad et al. [60] for sugar beet pulp (~1 meq g^{-1}), suggesting that bergamot pomace contains a greater amount of acidic functional groups compared to other biomasses. The ratio between the site concentration values obtained in this work is about one, whereas that determined for lemon pectin peels is about two and is in favour of the carboxylate groups. Interestingly, the refined concentration for POM_1 and POM_2 resulted very close. Similar conclusions were drawn also by means of the FOCUS approach [61]: the pK_a spectrum obtained for the P1-a aliquot displayed two peaks with maxima at p$K_{a1} = 3.60$ and p$K_{a2} = 10.80$, whose sites concentrations is equal to 0.72 and 0.77 meq g^{-1}, respectively (Fig. S3). On these bases, it may be inferred that the two sites belong to the same polyelectrolyte.

Data obtained for acidic constants and site concentrations are in a very good agreement within all pretreatments, thus values referring to the last line of Table 1 were used during the data analysis of potentiometric titrations aimed at the study on the complexing ability towards Cd^{2+}. Since it is well known that chloride forms quite stable species with Cd^{2+}, measurements were carried out in $NaNO_{3(aq)}$ (at $I = 0.10$ mol dm^{-3} and $t = 25$ °C) to avoid competition between chloride and pomace functional groups for cadmium(II) complexation.

The elaboration of potentiometric titrations was performed in the pH range 2.0–10.5 by keeping constant the acidic constants of POM_1 and POM_2 and the cadmium hydrolysis constants [62,63]. Moreover, the site concentration values were kept fixed during the data analysis and computed from the mass of the sorbent considering that $[POM_1] = 0.97$ meq g^{-1} and $[POM_2] = 1.00$ meq g^{-1}.

The results of the data analysis evidenced the presence of three complex species, namely $Cd(POM_1)(POM_2)H^+$, $Cd(POM_1)(OH)^0$, and $Cd(POM_2)(OH)^0$, whose formation constant values resulted to be $\log\beta_{Cd(POM_1)(POM_2)H} = 16.20 \pm 0.04$, $\log\beta_{Cd(POM_1)OH} = -5.15 \pm 0.03$, and $\log\beta_{Cd(POM_2)OH} = -6.26 \pm 0.03$. The inclusion of other species, such as Cd(POM_2)H and $Cd_2(POM_2)$, was also tested but the software failed to reach convergence. Selection criteria already reported in the literature [64,65] were used to choose the final speciation model. The distribution diagram displayed in Fig. 2 indicates that pomace functional sites are able to coordinate Cd^{2+} cation in the whole investigated pH range, being more efficient with increasing pH. In the selected conditions, the formation of the protonated species achieves about 40% of formation percentage in the typical pH range of natural fluids (*i.e.*, 4.0 < pH < 8.5). The stoichiometry of this species also suggests that in acidic conditions both sites cooperate for the coordination of Cd^{2+} cation. On the contrary, as the deprotonation of the POM_1 begins, at pH ~ 9, the speciation changes and the two sites can coordinate Cd^{2+} separately, trough mixed hydrolytic species.

To have an indication of the stability of each species in a more traditional feature, the formation constants could be rearranged using the acidic and the cadmium first hydrolysis constants ($\log K^{H}_{POM_1} = 10.69$ and $\log K^{*}_{Cd(OH)} = -10.31$) as follows:

$$Cd^{2+} + HPOM_1 + POM_2^- = Cd(HPOM_1)(POM_2)^+ \quad \log\beta = 16.20 - 10.69 = 5.51 \quad (5)$$

$$Cd(OH)^+ + POM_1^- = (CdOH)(POM_1)^0 \quad \log\beta = -5.15 - (-10.31) = 5.16 \quad (6)$$

$$Cd(OH)^+ + POM_2^- = (CdOH)(POM_2)^0 \quad \log\beta = -6.26 - (-10.31) = 4.05 \quad (7)$$

Above values give a better idea of the real strength with which pomace functional groups may coordinate Cd^{2+}. In the literature, there is only the value given by Cataldo et al. [66], reporting log $K = 3.35$ and 3.68 for the CdL species (L stands for pure commercial pectin and polygalacturonic acid, respectively) as well as log $\beta = 7.55$ and 7.77 for the CdHL species (same order).

Considering the differences in the matrix and in the data treatment (Cataldo et al. adopted the diprotic like model [67] and limited the pH range from 2 to 7) the values can be considered in a reasonably good agreement. The data reported in this section indicate that *dry* bergamot pomace is able to efficiently bind Cd(II) in the whole pH range of natural waters (4 ≤ pH ≤ 9). Moreover, the density of sorbent sites available for ionic exchange was quantified.

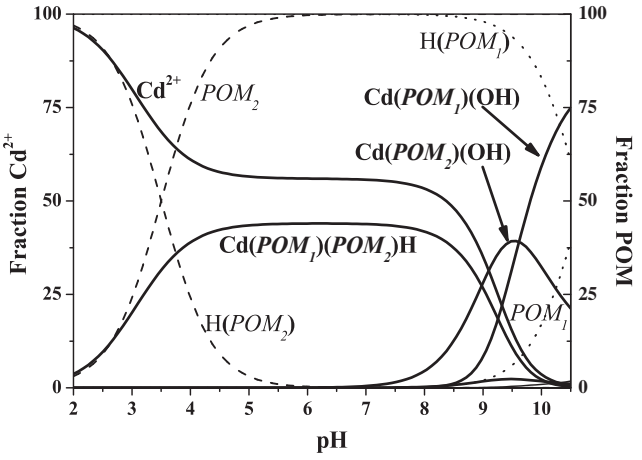

Fig. 2. Distribution diagram of Cd(II) species (solid lines) in the presence of pomace sorbent in $NaNO_{3(aq)}$. Experimental conditions: $I = 0.10$ mol dm^{-3}, $t = 25$ °C, $c^{2+}_{Cd} = 1$ mmol dm^{-3}; $c_{POM1} = c_{POM2} = 2$ mmol dm^{-3}. Dotted and dashed lines represent the protonation state of POM_1 and POM_2, respectively.

3.4. Cd^{2+} sorption tests

As showed in Fig. 3, the best data fitting for kinetic experiments was obtained employing a PSO (solid line) kinetics model (Table S6, eq. (2) and the time required to reach the equilibrium is 1 h.

It is worth to mention that from the literature it is known that for similar kinds of sorbents the equilibria between the solid phase and the target analyte in solution display a PSO kinetics behaviour [26,47,56,68–71]. The time required to reach equilibrium was found to be between 30 min and 2 h.

The sorption capacity of the different P1-a ÷ P1-f aliquots was evaluated by batch experiments (see details in Table S3) by measuring C_e and Q_e parameters (eq. (3) as well as the pH of the solutions before adding the sorbent ($pH_0 \sim 5.50$) and at equilibrium (pH_e). As a common feature, for all the investigated samples it was observed that $pH_e < pH_0$ (Fig. S4). Conversely, for the P1-c aliquot, pretreated with NaOH, pH_e was quite similar to pH_0 for all the solutions. This behaviour was explained considering that on one side P1-c sample is deprotonated so that the interaction with Cd^{2+} may occur without proton displacement, whereas all the other aliquots undergo deprotonation of acidic groups upon Cd^{2+} sorption. Moreover, this hypothesis is supported by the evidence that the difference between pH_0 and pH_e increases as a function of the sorbent amount. Therefore, the equation (eq. (8) reported by Schiewer et al. [59] was used, in order to take into account the pH variation and the above reported sorbent acidic constants:

$$Q_e = \frac{Q_{MAX} \cdot K^{Cd} \cdot C_e}{1 + [H^+] \cdot K^H_{POM1} + [H^+] \cdot K^H_{POM2} + K^{Cd} \cdot C_e} \quad (8)$$

where K^{Cd} is the Cd^{2+}/sorbent binding constant, $K^{H}_{POM_1}$ e $K^{H}_{POM_2}$ are the acidic constants and the $[H^+]$ is obtained from pH_e (Fig. S4).

The data obtained using eq. (8), listed in Table 2, resulted to be satisfying for all the pomace fractions.

The Cd(II) sorption capacity calculated for each single pomace aliquots resulted in the range $Q_{MAX} = 100–207$ mg g^{-1}, corresponding to 0.89–1.85 mmol g^{-1} of metal sorbed. These values suggest a higher pomace adsorption capacity for Cd^{2+} sequestration with respect to orange, lemon, pomelo, grapefruit peel or other citrus waste-based materials reported in literature, whose data are reported in Table 3. Nevertheless, analysing simultaneously the data obtained for the P1-a ÷ P1-f fractions (Table 2), a more robust estimation of the cadmium sorption capacity is $Q_{MAX} = 92 \pm 7$ mg g^{-1}, namely 0.82 mmol g^{-1}. These results are in agreement both with the total sites concentration

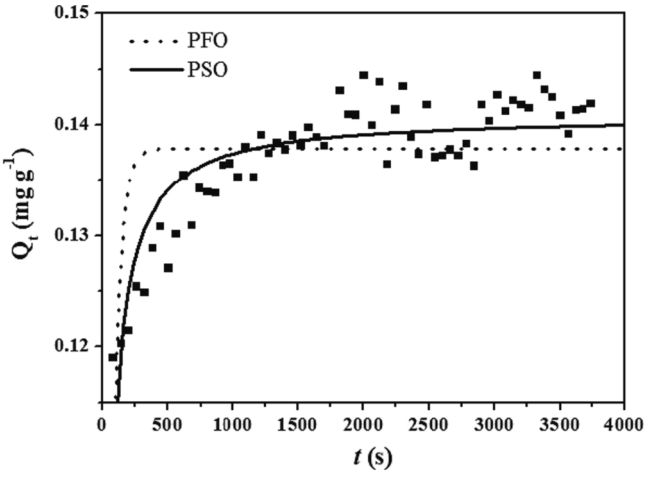

Fig. 3. Scatter plot of Cd^{2+}/P1-a aliquot sequestration kinetics data fitted using Pseudo Fist Order (PFO, dotted line) and Pseudo Second Order (PSO, solid line) equations. Experimental conditions: $c_{Cd(II)} = 0.40$ mg dm^{-3}, $m_{P1\text{-}a} = 30$ mg, $I = 0.10$ mol dm^{-3} in $NaNO_{3(aq)}$, $t = 25$ °C.

Table 2
Equilibrium constant ($\log K^{Cd}$) and Q_{MAX} values determined for the different P1-a ÷ P1-f aliquots by using eq. (8) [59] and mmoles of Cd^{2+} sorbed by pretreated pomace.

Pomace aliquot (pretreatment)	log K^{Cd}	Q_{MAX} (mg g^{-1})	mmol$^{2+}_{sorbed}$ g^{-1}
P1-a (H_2O)	5.44 ± 0.25[a)]	207 ± 45[a)]	1.85
P1-b (H_2O, $t = 100$ °C)	4.87 ± 0.16	189 ± 44	1.69
P1-c (NaOH)	4.39 ± 0.15	191 ± 49	1.70
P1-d (HNO_3)	5.41 ± 0.10	100 ± 12	0.89
P1-e (H_2O_2)	5.50 ± 0.10	125 ± 14	1.12
P1-f (2-propanol)	5.01 ± 0.03	134 ± 6	1.20
P1-a ÷ P1-f pretreatments	5.43 ± 0.08	92 ± 7	0.82

[a)] ± std. dev.

Table 3
Biosorption capacities of various sorbent materials for Cd(II) sequestration.

Sorbent material	Q_{MAX} (mg g^{-1})	Ref.
Orange peel	170	[73]
Orange peel [a)]	126	[74]
Orange peel	124	[71]
Orange peel	63	[75]
Orange peel	42	[48]
Orange peel	36	[76]
Orange peel [b)]	14	[56]
Orange peel	4	[77]
Orange waste	45	[47]
Lemon peel [c)]	182	[78]
Lemon peel [d)]	172	[78]
Lemon peel [e)]	118	[78]
Lemon peel [f)]	81	[58]
Lemon peel	55	[48]
Pomelo peel	22	[79]
Grapefruit peel	42	[54]
***Dry* bergamot pomace**	**92 ± 7 [g)]**	**This work**

[a)] pretreated with $(C_2H_5)OH$ + NaOH 0.50 mol dm^{-3} + KCl 1.00 mol dm^{-3}; [b)] pretreated with HNO_3 0.10 mol dm^{-3}; [c)] pretreated with NaOH 0.10 mol dm^{-3} + oxalic acid 0.10 mol dm^{-3}; [d)] pretreated with NaOH 0.10 mol dm^{-3}; [e)] pretreated with oxalic acid 0.10 mol dm^{-3}; [f)] NaOH 0.10 mol dm^{-3}; [g)] ± std. dev.

obtained in the case of the pomace acid-base investigation (*i.e.,* ~ 1.0 meq g^{-1}, Table 1) as well as with, for example, the data reported by Lodeiro et al. [71] who determined a $Q_{MAX} = 124$ mg g^{-1} and 1.10 mmol g^{-1} sorbed, using orange peel as biosorbent material.

Moreover, data in Table 2 suggest that, among the procedures tested, the pretreatment of *dry* pomace with water at 30 °C can be considered the one that actually leads to the material (P1-a) with the most significant Cd^{2+} sorption efficiency, as well as the most eco-friendly and sustainable.

Interestingly, the value of $\log K^{Cd}$ reported in Table 2 (5.43 ± 0.08) is similar to the value determined by potentiometry and given in eq. (5) ($\log \beta = 5.51$) as the measure of the binding affinity in the acidic pH range.

An indication about the Cd^{2+}/sorbent interaction is gained by looking at Fig. S5 where the ATR FT-IR spectrum of P1-c fraction (pH ~ 5.3) is compared to the one recorded on the same aliquot after contacting with the metal cation to perform the Cd^{2+} sorption tests, at similar pH value. The main differences between the two profiles are changes in the position and intensity of the signals assigned to the –OH groups possibly arising from pectin alcohol and carboxylic acid groups and from cellulose hydroxylic groups at about 3320 cm^{-1} [47], and to the asymmetric stretching vibrations of COO^- [49,50] at around 1610 cm^{-1}, as well as the peak owing the C-O-C stretching from cellulose at about 895 cm^{-1} [55].

Several authors reported that the difference (shift, Δ) between the asymmetric ($\upsilon_{a(COO-)}$) and symmetric ($\upsilon_{s(COO-)}$) stretching frequencies of ionic COO^- groups in absence and in the presence of metal cations, can

provide information about the coordination mode, thus allowing to discriminate among monodentate, bidentate (chelation) and bridging complexes [51,52,72]. Unfortunately, the Δ values calculated using the information gained from P1-a ÷ P1-f samples spectra and the corresponding ones recorded in presence of Cd^{2+} did not allow to unambiguously differentiate between the formation of monodentate or bidentate complexes.

3.5. Cd^{2+} desorption tests

Different desorbing agents were selected to investigate the Cd^{2+} release from the bergamot pomace and evaluate the biosorbent stability and reusability for multiple loading/desorption cycles [26,80], without any significant adsorption and stripping effectiveness losses [58,81]. The P1-a pomace fraction was chosen to perform the desorption experiments since it resulted the one affording the most significant Cd^{2+} sorption (section 3.4.). Inorganic acids (HCl, HNO_3) and chelating agents (EDTA, biodegradable L-GLDA and S,S-EDDS) were selected for carrying out the stripping tests, owing to their known efficient capability in cadmium(II) desorption from citrus [39,58] and algal [82] biomasses binding sites [81], as well as for the metal remediation from soils [83,84]. The L-GLDA, S,S-EDDS, EDTA solutions to be employed for the elution experiments, were prepared in the pH range 8.5–9.5, where the maximum possible Cd^{2+} sequestering ability is observed for the three chelating agents [85] and, at the same time, to hinder the metal cation hydrolysis [62,63].

In detail, stripping experiments were performed on pomace loaded with Cd^{2+}, selecting different eluent concentrations (0.008, 0.10 mol dm^{-3}), various temperatures (25, 45 °C) and contact times (30, 60 min). The stripping efficiency *DE* (%) was calculated at each experimental condition by means of eq. (4). The best results were achieved by inorganic acids and EDTA with maximum desorption efficiencies of 60 % for a single cycle. Biodegradable ligands showed a lower efficiency, reaching values around 40 % after the first cycle.

The *DE* data were modelled as a function of temperature, eluent concentration and time of contact by means of multilinear regression after column autoscaling. Models so obtained, one for each desorbing agent, were cross-validated (CV) and the evaluation was performed by looking at RMSECV (root mean square error in cross-validation) and percentage of explained variance both in fitting and in cross-validation. The parameters of the models, together with their significance, and the evaluation statistics are summarized in Table S7. Models can be considered reliable (RMSECV values are quite low), even if that of L-GLDA has a very low explained variance in CV. This is explained by the very low variability of the *DE* in the experimental domain, the three parameters have almost the same value and none of them is statistically significant at 95% C.I. As a general trend, temperature has a negative effect on *DE* (except for HCl), indicating that low temperatures provide a more efficient desorption than high ones. This is likely related to the enthalpy change of complex formation reactions in solution. Available data in the NIST database [86] confirm this behavior, since Cd^{2+}/Cl^- complexes are slightly endothermic (*e.g.*, stepwise ΔH for the formation of $CdCl^+$, $CdCl_2$ and $CdCl_3^-$ species are about 2, 2 and 4 kJ mol^{-1}, respectively), whereas Cd^{2+}/EDTA ones are largely exothermic (*e.g.*, ΔH for the formation of $CdEDTA^{2-}$ species is −38 kJ mol^{-1}).

Ligand concentration and, to a lower extent, time of contact feature the opposite trend. EDTA model was built after elimination of an outlier (ID n. 3) and shows a negative value for the parameter b2 corresponding to the ligand concentration. This is difficult to explain and may deserve further investigations.

3.6. Determination of phenolic and oxygenated heterocyclic compounds in washing solutions from pretreated pomace

The washing solutions obtained from different pomace pretreatment (P1-a ÷ P1-f) were injected after proper dilution (1:10 with water for all samples). Concerning the bioactive content in terms of phenolic acid and flavonoids, their chromatographic profile for the sample P1-a is shown in Fig. S6.

The compounds were identified based on complementary information from the PDA and MS spectra in combination with data already reported in the literature. Two phenolic acids and twelve flavonoids were positively detected and quantified. A detailed list of the identified and quantified (after conversion from mg L^{-1} to mg kg^{-1} of the sample) compounds of all the sample analysed are shown in the Table 4.

As the result, all sample showed very similar qualitative profile, but P1-a was the quantitative richest in bioactive molecules (15133.02 ± 243.31 mg kg^{-1}) followed by P1-f (14695.36 ± 48.65 mg kg^{-1}) whereas P1-b was the quantitative poorest in molecules of the biological interest (1298.97 ± 7.43 mg kg^{-1}). More in details, neoeriocitrin, naringin and neohesperidin that have inflammatory activity [87,88] were the most abundant compounds in all samples, on the contrary C-glucosidic compounds were the minority compounds. Furthermore, the presence in high amounts of two important compounds such as melitidin and brutieridin, which showed hypolipidemic [89], confirmed the beneficial effects on human health.

The same samples were subsequently injected for the elucidation of the oxygenated heterocyclic content. The MRM chromatograms obtained (data not shown) are consistent with a residual presence of OHCs compound related to bergamot. For each pretreatment, qualitative and quantitative results, expressed as mg kg^{-1} of dried pomace ± standard deviation, are reported in Table S8.

Fourteen compounds were positively identified and among them, three were coumarins, six were furocoumarins and five were polymethoxyflavones. The highest sensitivity of the MRM detection led to quantify even minor components, which were not commonly revealed through the spectrophotometric detector, as suggested by comparison of these results with those obtained by Russo *et al.* in which OHCs in various bergamot samples (peel, pulp, seed and juice) were identified and quantified by means of RP-HPLC with both UV and MS single quadrupole detectors [24]. The highest amount of OHCs was found for sample P1-b treated with water at $t = 100$ °C; however, it should be noted that five compounds (isopimpinellin, sinensetin, epoxybergamottin and 5-O-demethyltangeretin and 6′,7′-dihydroxybergamottin) were not detected when using this pomace pretreatment. Furthermore, the lower amount of bergamottin (6.64 ± 0.19 mg kg^{-1}), the absence of 6′,7′-dihydroxybergamottin and the simultaneous increase of bergapten (433.07 ± 1.90 mg kg^{-1}) is in accordance with the results obtained after heat treatment of grapefruit juice by Uesawa et al. [90]. All the other treatments, seems to have less influence on the total OHCs content, with results varying from 200.94 ± 1.44 for sample P1-c to 307.52 ± 4.56 mg kg^{-1} for sample P1-e, only due to minor variation of some of the investigated compounds, like the values obtained for 6′,7′-dihydroxybergamottin in sample P1-e. The latter could be explained by an opening of the epoxy ring of epoxybergamottin in this medium.

4. Conclusions

For the first time, a comprehensive strategy to assess the potential of exploiting bergamot waste coming from citrus agri-food supply chain to develop biobased sustainable materials able to efficiently sequester cadmium(II) from aqueous solution as well as to recover added-value biomolecules has been here studied.

From the data collected, pretreated bergamot pomace is capable to remove a maximum Cd(II) amount, at pH ~ 5, of 207 ± 45 mg g^{-1}, however a more robust estimation of this parameter is 92 ± 7 mg g^{-1}. The acidic and cadmium(II) complex formation constants indicate that *dry* bergamot pomace may efficiently bind Cd(II) in the whole pH of natural waters ($4 \leq pH \leq 9$).

Stripping tests aimed at evaluating the possibility of reusing the biobased sorbent were carried out at different experimental conditions, optimized by means of a full factorial experimental design. The

Table 4
Qualitative and quantitative results for phenolic acids and flavonoids compounds (in mg kg^{-1}). Results are reported as the average of three replicate measurements.

N°	Compound	Retention time (min)	λ (nm)	$[M-H]^-$/ $[M+H]^+$	P1-a (H_2O)	P1-b (H_2O, $t = 100$ °C)	P1-c (NaOH)	P1-d (HNO_3)	P1-e (H_2O_2)	P1-f (2-propanol)
1	Ferulic acid 4-O-glucoside	12.15 ± 0.43[a)]	218–327	355/-	<LOQ	<LOQ	<LOQ	<LOQ	<LOQ	<LOQ
2	Sinapoyl glucose	13.48 ± 0.45	287–324	385/-	<LOQ	<LOQ	<LOQ	<LOQ	<LOQ	<LOQ
3	Apigenin-dihexoside	17.49 ± 0.49	270–335	593/595	186.83 ± 6.06[a)]	<LOQ	154.09 ± 8.86[a)]	172.49 ± 1.00[a)]	137.85 ± 7.66[a)]	172.44 ± 0.52[a)]
4	Diosmetin-diexoside	20.21 ± 0.50	270–347	623/625	83.70 ± 2.23	13.27 ± 0.16	80.72 ± 9.60	78.29 ± 0.58	95.25 ± 8.53	77.88 ± 0.27
5	Eriocitrin	23.53 ± 0.74	284	595/-	64.56 ± 6.72	<LOQ	–	56.83 ± 0.01	58.00 ± 11.00	57.32 ± 0.22
6	Neoeriocitrin	23.95 ± 0.41	286	595/-	3417.50 ± 94.53	293.92 ± 0.85	3142.98 ± 12.22	3195.11 ± 14.62	2004.89 ± 104.30	3282.03 ± 11.67
7	Poncirin	27.32 ± 0.38	207–349	593/595	79.23 ± 11.60	12.29 ± 0.24	94.37 ± 3.27	85.67 ± 0.08	121.04 ± 15.10	88.36 ± 0.01
8	Diosmetin 8-C-glucoside	28.10 ± 0.39	270–344	461/463	21.13 ± 0.15	13.27 ± 0.16	18.73 ± 0.51	21.03 ± 0.49	32.53 ± 2.74	22.39 ± 0.07
9	Naringin	28.41 ± 0.35	216–283-328	579/-	4405.09 ± 70.60	407.61 ± 2.85	4310.47 ± 44.13	4132.15 ± 17.04	2556.05 ± 373.08	4291.68 ± 11.58
10	Apigenin 7-O-neohesperidoside	30.94 ± 0.33	208–266-336	577/579	277.15 ± 6.25	<LOQ	243.29 ± 13.24	238.40 ± 1.36	258.47 ± 12.81	279.72 ± 1.75
11	Neohesperidin	31.47 ± 0.35	283–325	609/-	3438.88 ± 19.19	314.86 ± 0.35	3329.87 ± 11.58	2054.75 ± 4.16	1960.18 ± 11.50	3335.92 ± 8.13
12	Neodiosmin	33.32 ± 0.35	265–344	607/609	93.61 ± 4.27	11.49 ± 0.02	88.82 ± 12.63	87.75 ± 0.64	101.14 ± 19.76	92.34 ± 4.60
13	Melitidin	36.08 ± 0.31	220–283-329	723/-	848.90 ± 13.12	53.07 ± 0.74	793.49 ± 3.42	786.35 ± 2.00	424.55 ± 172.84	841.50 ± 2.38
14	Brutieridin	38.27 ± 0.33	283–327	753/-	2216.44 ± 8.58	179.19 ± 0.17	2094.43 ± 117.46	2054.65 ± 4.16	1507.37 ± 110.45	2153.78 ± 7.45
	Total of biomolecules				**15133.02 ± 243.31**	**1298.97 ± 7.43**	**14351.26 ± 236.87**	**12963.47 ± 46.15**	**9257.32 ± 849.79**	**14695.36 ± 48.65**

[a)] ± std. dev.

experiments revealed that the most efficient desorbents resulted to be HCl, HNO_3 and EDTA (~60 % for a single cycle), although *DE* obtained with the biodegradable L-GLDA and S,S-EDDS are interesting (~40 % for a single cycle).

Since the amount of Cd^{2+} sorbed (~0.8 mmol g^{-1}) and the individual site concentration (~1.0 meq g^{-1}) are very similar, it could be inferred that the mechanism involved is the ionic exchange.

On the other hand, the analyses carried out on the solutions recovered after the pomace pretreatments revealed that, among phenolic composition, the sample pretreated with water at $t = 30$ °C contained the highest amount of biomolecules (15133.02 ± 243.31 mg kg^{-1}), followed by sample pretreated with 2-propanol (14695.36 ± 48.65 mg kg^{-1}). Conversely, sample pretreated by H_2O at $t = 100$ °C contained the lowest amount (1298.97 ± 7.43 mg kg^{-1}). As regards OHCs, values were in the range of 200–300 mg kg^{-1} for all the treatments except for the sample pretreated with H_2O at $t = 100$ °C in which a total OHCs content of 572.65 ± 12.99 mg kg^{-1} was found. From the yield measured in this paper, about 15 kg of bergamot pomace are required to obtain 1 kg of active biomass and 15 g of bioactive molecules.

In conclusion, the results have shown that the pretreatment of *dry* bergamot pomace with water at a temperature of 30 °C proved to be highly effective. This method yielded a solid sorbent that exhibited excellent efficiency in removing Cd(II) from aqueous solutions. Additionally, this approach presents a feasible strategy for extracting healthful nutraceuticals in the food industry.

Funding

The work presented in this paper was partially funded by European Union – FSE-REACT-EU, PON Ricerca e Innovazione 2014–2020, D.M. 1062/2021.

CRediT authorship contribution statement

Anna Irto: Investigation, Data curation, Formal analysis, Validation, Visualization, Writing – original draft, Writing – review & editing. **Salvatore Giovanni Michele Raccuia:** Investigation, Data curation, Formal analysis. **Gabriele Lando:** Conceptualization, Formal analysis, Data curation, Methodology, Validation, Writing – original draft, Writing – review & editing, Software. **Concetta De Stefano:** Conceptualization, Resources, Funding acquisition, Software, Validation. **Katia Arena:** Investigation, Data curation, Validation, Writing – original draft. **Tania Maria Grazia Salerno:** Investigation, Data curation, Validation, Writing – original draft. **Alberto Pettignano:** Investigation, Data curation, Validation. **Francesco Cacciola:** Data curation, Methodology, Writing – review & editing. **Luigi Mondello:** Resources, Funding acquisition, Validation. **Paola Cardiano:** Conceptualization, Data curation, Funding acquisition, Methodology, Writing – original draft, Writing – review & editing, Project administration, Supervision.

Declaration of Competing Interest

The authors declare that they have no known competing financial interests or personal relationships that could have appeared to influence the work reported in this paper.

Data availability

Data will be made available on request.

Appendix A. Supplementary data

Supplementary data to this article can be found online at https://doi.org/10.1016/j.microc.2023.109183.

References

[1] D. Panwar, A. Saini, P.S. Panesar, H.K. Chopra, Unraveling the scientific perspectives of citrus by-products utilization: progress towards circular economy, Trends Food Sci. Technol. 111 (2021) 549–562.

[2] S. Multari, S. Carlin, S. Vincenzo, S. Martens, Differences in the composition of phenolic compounds, carotenoids, and volatiles between juice and pomace of four citrus fruits from Southern Italy, Eur. Food Res. Technol. 246 (2020).
[3] K. Sharma, N. Mahato, M.H. Cho, Y.R. Lee, Converting citrus wastes into value-added products: Economic and environmently friendly approaches, Nutrition (Burbank Los Angeles County, Calif.) 34 (2017) 29–46.
[4] D.A. Zema, P.S. Calabrò, A. Folino, V. Tamburino, G. Zappia, S.M. Zimbone, Valorisation of citrus processing waste: a review, Waste Manag. 80 (2018) 252–273.
[5] B.R. Moser, C. Dorado, G.B. Bantchev, J.K. Winkler-Moser, K.M. Doll, Production and evaluation of biodiesel from sweet orange (Citrus sinensis) lipids extracted from waste seeds from the commercial orange juicing process, Fuel 342 (2023), 127727.
[6] S. Suri, A. Singh, P.K. Nema, Current applications of citrus fruit processing waste: A scientific outlook, Appl. Food Biotechnol. 2 (2022), 100050.
[7] N. Mahato, K. Sharma, M. Sinha, E.R. Baral, R. Koteswararao, A. Dhyani, M. Hwan Cho, S. Cho, Bio-sorbents, industrially important chemicals and novel materials from citrus processing waste as a sustainable and renewable bioresource: A review, J. Adv. Res. 23 (2020) 61–82.
[8] S. Caballero, Y.O. Li, D.J. McClements, G. Davidov-Pardo, Encapsulation and delivery of bioactive citrus pomace polyphenols: a review, Crit. Rev. Food Sci. Nutr. 62 (2022) 8028–8044.
[9] K. Kandemir, E. Piskin, J. Xiao, M. Tomas, E. Capanoglu, Fruit juice industry wastes as a source of bioactives, J. Agric. Food Chem. 70 (2022) 6805–6832.
[10] WHO, IPCS Cadmium, Cadmium Chloride, Cadmium Oxide, Cadmium Sulphide, Cadmium Acetate, Cadmium Sulphate, Geneva, Switzerland, 1992.
[11] UNEP, Final Review of Scientific Information on Cadmium; United Nations Environment Programme, 2010.
[12] F. Crea, C. Foti, D. Milea, S. Sammartano, Speciation of cadmium in the environment, Met. Ions Life Sci. 11 (2013) 63–83.
[13] M. Garside, Global refinery production of cadmium by country, 2021.
[14] J. Bayuo, M.J. Rwiza, M. Sillanpää, K.M. Mtei, Removal of heavy metals from binary and multicomponent adsorption systems using various adsorbents – a systematic review, RSC Adv. 13 (2023) 13052–13093.
[15] L. Joseph, B.-M. Jun, J.R.V. Flora, C.M. Park, Y. Yoon, Removal of heavy metals from water sources in the developing world using low-cost materials: A review, Chemosphere 229 (2019) 142–159.
[16] A. Othmani, S. Magdouli, P. Senthil Kumar, A. Kapoor, P.V. Chellam, Ö. Gökkuş, Agricultural waste materials for adsorptive removal of phenols, chromium (VI) and cadmium (II) from wastewater: A review, Environ. Res. 204 (2022), 111916.
[17] A. Badawi, M. Abd El-Kodous, G. Ali, Recent advances in dyes and metal ions removal using efficient adsorbents and novel nano-based materials: An overview, RSC Adv. 11 (2021) 36528–36553.
[18] M. Bilal, I. Ihsanullah, M. Younas, M. Ul Hassan Shah, Recent advances in applications of low-cost adsorbents for the removal of heavy metals from water: A critical review, Sep. Purif. Technol. 278 (2021), 119510.
[19] K. Gupta, P. Joshi, R. Gusain, O.P. Khatri, Recent advances in adsorptive removal of heavy metal and metalloid ions by metal oxide-based nanomaterials, Coord. Chem. Rev. 445 (2021), 214100.
[20] M.M. Kwikima, S. Mateso, Y. Chebude, Potentials of agricultural wastes as the ultimate alternative adsorbent for cadmium removal from wastewater. A review, Sci. Afr. 13 (2021) e00934.
[21] J. Sulejmanović, E. Skopak, E. Šehović, A. Karadža, A. Zahirović, N. Smječanin, O. Mahmutović, S. Ansar, F. Sher, Surface engineered functional biomaterials for hazardous pollutants removal from aqueous environment, Chemosphere 336 (2023), 139205.
[22] T. Arsenie, I.G. Cara, M.-C. Popescu, I. Motrescu, L. Bulgariu, Evaluation of the adsorptive performances of rapeseed waste in the removal of toxic metal ions in aqueous media, Water 14 (2022) 4108.
[23] L. Bulgariu, D.I. Ferţu, I.G. Cara, M. Gavrilescu, Efficacy of alkaline-treated soy waste biomass for the removal of heavy-metal ions and opportunities for their recovery, Materials (Basel Switzerland) 14 (2021).
[24] M. Russo, A. Arigò, M.L. Calabrò, S. Farnetti, L. Mondello, P. Dugo, Bergamot (Citrus bergamia Risso) as a source of nutraceuticals: limonoids and flavonoids, J. Funct. Foods 20 (2016) 10–19.
[25] S. Schiewer, A. Balaria, Biosorption of Pb^{2+} by original and protonated citrus peels: Equilibrium, kinetics, and mechanism, Chem. Eng. J. 146 (2009) 211–219.
[26] S. Schiewer, S.B. Patil, Pectin-rich fruit wastes as biosorbents for heavy metal removal: Equilibrium and kinetics, Bioresour. Technol. 99 (2008) 1896–1903.
[27] U. Suryavanshi, S.R. Shukla, Adsorption of Pb^{2+} by alkali-treated citrus limetta peels, Ind. Eng. Chem. Res. 49 (2010) 11682–11688.
[28] G. Costanzo, M.R. Iesce, D. Naviglio, M. Ciaravolo, E. Vitale, C. Arena, Comparative studies on different citrus cultivars: a revaluation of waste mandarin components, Antioxidants (Basel, Switzerland) 9 (2020) 517.
[29] H. Jiang, W. Zhang, Y. Xu, L. Chen, J. Cao, W. Jiang, An advance on nutritional profile, phytochemical profile, nutraceutical properties, and potential industrial applications of lemon peels: A comprehensive review, rends, Food Sci. Technol. 124 (2022) 219–236.
[30] B. Singh, J.P. Singh, A. Kaur, N. Singh, Phenolic composition, antioxidant potential and health benefits of citrus peel, Food Res. Int. 132 (2020), 109114.
[31] E. Sommella, G. Pepe, F. Pagano, G.C. Tenore, S. Marzocco, M. Manfra, G. Calabrese, R.P. Aquino, P. Campiglia, UHPLC profiling and effects on LPS-stimulated J774A.1 macrophages of flavonoids from bergamot (*Citrus bergamia*) juice, an underestimated waste product with high anti-inflammatory potential, J. Funct. Foods 7 (2014) 641–649.
[32] A. Zayed, M.T. Badawy, M.A. Farag, Valorization and extraction optimization of Citrus seeds for food and functional food applications, Food Chem. 355 (2021), 129609.
[33] A. Arigò, P. Dugo, F. Rigano, L. Mondello, Linear retention index approach applied to liquid chromatography coupled to triple quadrupole mass spectrometry to determine oxygen heterocyclic compounds at trace level in finished cosmetics, J. Chromatogr. A 1649 (2021), 462183.
[34] P. Cardiano, C. Foti, O. Giuffrè, On the interaction of N-acetylcysteine with Pb^{2+}, Zn^{2+}, Cd^{2+} and Hg^{2+}, J. Mol. Liq. 223 (2016) 360–367.
[35] R.M. Cigala, C. De Stefano, A. Irto, D. Milea, S. Sammartano, Thermodynamic data for the modeling of lanthanoid(III) Sequestration by reduced glutathione in aqueous solution, J. Chem. Eng. Data 60 (2015) 192–201.
[36] F. Crea, C. De Stefano, A. Irto, G. Lando, S. Materazzi, D. Milea, A. Pettignano, S. Sammartano, Understanding the solution behavior of epinephrine in the presence of toxic cations: a thermodynamic investigation in different experimental conditions, Molecules 25 (2020).
[37] G. Blanchard, M. Maunaye, G. Martin, Removal of heavy metals from waters by means of natural zeolites, Water Res. 18 (1984) 1501–1507.
[38] R. Leardi, Experimental design in chemistry: A tutorial, Anal. Chim. Acta 652 (2009) 161–172.
[39] E. Njikam, S. Schiewer, Optimization and kinetic modeling of cadmium desorption from citrus peels: A process for biosorbent regeneration, J. Hazard. Mat. 213–214 (2012) 242–248.
[40] A. Arigò, F. Rigano, G. Micalizzi, P. Dugo, L. Mondello, Oxygen heterocyclic compound screening in Citrus essential oils by linear retention index approach applied to liquid chromatography coupled to photodiode array detector, Flavour, Fragance J. 34 (2019) 349–364.
[41] C. De Stefano, S. Sammartano, P. Mineo, C. Rigano, Computer tools for the speciation of natural fluids, in: A. Gianguzza, E. Pelizzetti, S. Sammartano (Eds.), Marine Chemistry - An Environmental Analytical Chemistry Approach, Kluwer Academic Publishers, Amsterdam, 1997, pp. 71–83.
[42] P. Cardiano, C. Foti, F. Giacobello, O. Giuffrè, S. Sammartano, Study of Al^{3+} interaction with AMP, ADP and ATP in aqueous solution, Biophys. Chem. 234 (2018) 42–50.
[43] L. Alderighi, P. Gans, A. Ienco, D. Peters, A. Sabatini, A. Vacca, Hyperquad simulation and speciation (HySS): a utility program for the investigation of equilibria involving soluble and partially soluble species, Coord. Chem. Rev. 184 (1999) 311–318.
[44] A. Irto, P. Cardiano, S. Cataldo, K. Chand, R.M. Cigala, F. Crea, C. De Stefano, G. Gattuso, N. Muratore, A. Pettignano, S. Sammartano, M.A. Santos, Speciation studies of bifunctional 3-hydroxy-4-pyridinone ligands in the presence of Zn^{2+} at different ionic strengths and temperatures, Molecules 24 (2019) 4084.
[45] J.I. Lachowicz, G. Dalla Torre, R. Cappai, E. Randaccio, V.M. Nurchi, R. Bachor, Z. Szewczuk, L. Jaremko, M. Jaremko, M.B. Pisano, S. Cosentino, G. Orrù, A. Ibba, J. Mujika, X. Lopez, Metal self-assembly mimosine peptides with enhanced antimicrobial activity: towards a new generation of multitasking chelating agents, Dalton Trans. 49 (2020) 2862–2879.
[46] V.M. Nurchi, R. Cappai, N. Spano, G. Sanna, A friendly complexing agent for spectrophotometric determination of total iron, Molecules 26 (2021).
[47] A.B. Pérez-Marín, V.M. Zapata, J.F. Ortuño, M. Aguilar, J. Sáez, M. Lloréns, Removal of cadmium from aqueous solutions by adsorption onto orange waste, J. Hazard. Mater. 139 (2007) 122–131.
[48] M. Thirumavalavan, Y.-L. Lai, J.-F. Lee, Fourier transform infrared spectroscopic analysis of fruit peels before and after the adsorption of heavy metal ions from aqueous solution, J. Chem. Eng. Data 56 (2011) 2249–2255.
[49] M. Iqbal, S. Schiewer, R. Cameron, Mechanistic elucidation and evaluation of biosorption of metal ions by grapefruit peel using FTIR spectroscopy, kinetics and isotherms modeling, cations displacement and EDX analysis, J. Chem. Technol. Biotechnol. 84 (2009) 1516–1526.
[50] S. Schiewer, M. Iqbal, The role of pectin in Cd binding by orange peel biosorbents: A comparison of peels, depectinated peels and pectic acid, J. Hazard. Mater. 177 (2010) 899–907.
[51] P.X. Sheng, Y.P. Ting, J.P. Chen, L. Hong, Sorption of lead, copper, cadmium, zinc, and nickel by marine algal biomass: characterization of biosorptive capacity and investigation of mechanisms, J. Colloid Interface Sci. 275 (2004) 131–141.
[52] A. Carrasquero, F. Iraima, Cadmium binding by humic acids: an experiment in FTIR spectroscopy and soil chemistry, Chem. Educ. 9 (2004).
[53] V.-P. Dinh, T.-D.-T. Huynh, H.M. Le, V.-D. Nguyen, V.-A. Dao, N.Q. Hung, L. A. Tuyen, S. Lee, J. Yi, T.D. Nguyen, L.V. Tan, Insight into the adsorption mechanisms of methylene blue and chromium(III) from aqueous solution onto pomelo fruit peel, RSC Adv. 9 (2019) 25847–25860.
[54] M. Torab-Mostaedi, M. Asadollahzadeh, A. Hemmati, A. Khosravi, Equilibrium, kinetic, and thermodynamic studies for biosorption of cadmium and nickel on grapefruit peel, J. Taiwan Inst. Chem. Eng. 44 (2013) 295–302.
[55] J. Zhuang, M. Li, Y. Pu, A.J. Ragauskas, C.G. Yoo, Observation of Potential Contaminants in Processed Biomass Using Fourier Transform Infrared Spectroscopy, Appl. Sci., 10 (2020) 4345.
[56] M.R. Lasheen, N.S. Ammar, H.S. Ibrahim, Adsorption/desorption of Cd(II), Cu(II) and Pb(II) using chemically modified orange peel: Equilibrium and kinetic studies, Solid State Sci. 14 (2012) 202–210.
[57] F.T. Li, H. Yang, Y. Zhao, R. Xu, Novel modified pectin for heavy metal adsorption, Chin. Chem. Lett. 18 (2007) 325–328.
[58] M. Villen-Guzman, M.M. Cerrillo-Gonzalez, J.M. Paz-Garcia, J.M. Rodriguez-Maroto, B. Arhoun, Valorization of lemon peel waste as biosorbent for the simultaneous removal of nickel and cadmium from industrial effluents, Environ. Technol. Innov. 21 (2021), 101380.

[59] S. Schiewer, S.B. Patil, Modeling the effect of pH on biosorption of heavy metals by citrus peels, J. Hazard. Mater. 157 (2008) 8–17.
[60] Z. Reddad, C. Gérente, Y. Andrès, M.-C. Ralet, J.-F. Thibault, P. Le Cloirec, Ni(II) and Cu(II) binding properties of native and modified sugar beet pulp, Carbohydr. Polym. 49 (2002) 23–31.
[61] D.S. Smith, F.G. Ferris, Proton binding by hydrous ferric oxide and aluminum oxide surfaces interpreted using fully optimized continuous pK_a spectra, Environ. Sci. Technol. 35 (2001) 4637–4642.
[62] F. Crea, D. Milea, S. Sammartano, Enhancement of hydrolysis through the formation of mixed hetero-metal species: dioxouranium(VI) - cadmium(II) mixtures, Anal. Chim. 95 (2005) 767–778.
[63] C. Foti, G. Lando, F.J. Millero, S. Sammartano, Experimental study and modeling of inorganic Cd^{2+} speciation in natural waters, Environ. Chem. 8 (2011) 320–331.
[64] A. Irto, P. Cardiano, K. Chand, R.M. Cigala, F. Crea, C. De Stefano, L. Gano, G. Gattuso, S. Sammartano, M.A. Santos, A new bis-(3-hydroxy-4-pyridinone)-DTPA-derivative: Synthesis, complexation of di-/tri-valent metal cations and in vivo M^{3+} sequestering ability, J. Mol. Liq. 281 (2019) 280–294.
[65] A. Irto, P. Cardiano, K. Chand, R.M. Cigala, F. Crea, C. De Stefano, G. Gattuso, S. Sammartano, M.A. Santos, Complexation of environmentally and biologically relevant metals with bifunctional 3-hydroxy-4-pyridinones, J. Mol. Liq. 319 (2020), 114349.
[66] S. Cataldo, A. Gianguzza, A. Pettignano, D. Piazzese, S. Sammartano, Complex Formation of Copper(II) and Cadmium(II) with pectin and polygalacturonic acid in aqueous solution. An ISE-H^+ and ISE-Me^{2+} electrochemical study, Int. J. Electrochem. Sci. 7 (2012) 6722–6737.
[67] C. Bretti, R.M. Cigala, F. Crea, C. De Stefano, G. Gattuso, A. Irto, G. Lando, D. Milea, S. Sammartano, Thermodynamic Properties of O-Donor Polyelectrolytes: Determination of the Acid-Base and Complexing Parameters in Different Ionic Media at Different Temperatures, J. Chem. Eng. Data. 62 (2017) 2676–2688.
[68] S. Cataldo, A. Gianguzza, D. Milea, N. Muratore, A. Pettignano, S. Sammartano, A critical approach to the toxic metal ion removal by hazelnut and almond shells, Environ. Sci. Pollut. Res. 25 (2018) 4238–4253.
[69] S. Cataldo, A. Gianguzza, A. Pettignano, Sorption of Pd(II) ion by calcium alginate gel beads at different chloride concentrations and pH. A kinetic and equilibrium study, Arab. J. Chem. 9 (2016) 656–667.
[70] A. Jakóbik-Kolon, A. Milewski, K. Mitko, A. Lis, Preparation of pectin-based biosorbents for cadmium and lead ions removal, Sep. Sci. Technol. 49 (2014).
[71] P. Lodeiro, R. Herrero, M. Sastre de Vicente, Thermodynamic and kinetic aspects on the biosorption of cadmium by low cost materials: a review, Environ. Chem. 3 (2006) 400–418.
[72] C. Jeon, J.Y. Park, Y.J. Yoo, Biosorption model for binary adsorption sites, J. Microbiol. Biotechnol. 11 (2001) 781–787.
[73] Y. Chen, H. Wang, W. Zhao, S. Huang, Four different kinds of peels as adsorbents for the removal of Cd (II) from aqueous solution: kinetics, isotherm and mechanism, J. Taiwan Inst. Chem. Eng. 88 (2018) 146–151.
[74] X. Guo, S. Liang, Q. Tian, Removal of heavy metal ions from aqueous solutions by adsorption using modified orange peel as adsorbent, Adv. Mat. Res. 236–238 (2011) 237–240.
[75] N. Feng, X. Guo, S. Liang, Y. Zhu, J. Liu, Biosorption of heavy metals from aqueous solutions by chemically modified orange peel, J. Hazard. Mater. 185 (2011) 49–54.
[76] V.K. Gupta, A. Nayak, Cadmium removal and recovery from aqueous solutions by novel adsorbents prepared from orange peel and Fe_2O_3 nanoparticles, J. Chem. Eng. 180 (2012) 81–90.
[77] A.B. Pérez-Marín, J.F. Ortuño, M.I. Aguilar, V.F. Meseguer, J. Sáez, M. Lloréns, Use of chemical modification to determine the binding of Cd(II), Zn(II) and Cr(III) ions by orange waste, Biochem. Eng. J. 53 (2010) 2–6.
[78] M. Thirumavalavan, Y.-L. Lai, L.-C. Lin, J.-F. Lee, Cellulose-based native and surface modified fruit peels for the adsorption of heavy metal ions from aqueous solution: langmuir adsorption isotherms, J. Chem. Eng. Data 55 (2010) 1186–1192.
[79] W. Saikaew, P. Kaewsarn, W. Saikaew, Pomelo peel: agricultural waste for biosorption of cadmium ions from aqueous solutions, World Acad. Sci Eng. Technol. 3 (2009) 393–397.
[80] S. Cataldo, V. Chiodo, F. Crea, S. Maisano, D. Milea, A. Pettignano, Biochar from byproduct to high value added material – A new adsorbent for toxic metal ions removal from aqueous solutions, J. Mol. Liq. 271 (2018) 481–489.
[81] A. Chatterjee, J. Abraham, Desorption of heavy metals from metal loaded sorbents and e-wastes: A review, Biotechnol. Lett 41 (2019) 319–333.
[82] M. Kumar, A.K. Singh, M. Sikandar, Study of sorption and desorption of Cd (II) from aqueous solution using isolated green algae Chlorella vulgaris, Appl. Water Sci. 8 (2018) 225.
[83] V.M. Nurchi, R. Cappai, G. Crisponi, G. Sanna, G. Alberti, R. Biesuz, S. Gama, Chelating agents in soil remediation: a new method for a pragmatic choice of the right chelator, Front. Chem. 8 (2020), 597400.
[84] Z. Wei, Y. Chen, X. Li, H. Rong, Z. Huang, Remediation of heavy metal contaminated farmland soil by biodegradable chelating agent GLDA, Appl. Sci. 12 (2022) 9277.
[85] C. Bretti, R. Di Pietro, P. Cardiano, O. Gomez-Laserna, A. Irto, G. Lando, C. De Stefano, Thermodynamic solution properties of a biodegradable chelant (L-glutamic-N, N-diacetic Acid, L-GLDA) and its sequestering ability toward $C^{d2}+$, Molecules 26 (2021) 7087.
[86] A.E. Martell, R.M. Smith, R.J. Motekaitis, NIST Critically selected stability constants of metal complexes database, 8.0, National Institute of Standard and Technology, Garthersburg, MD, 2004.
[87] M. Jain, H.S. Parmar, Evaluation of antioxidative and anti-inflammatory potential of hesperidin and naringin on the rat air pouch model of inflammation, J. Inflamm. Res. 60 (2011) 483–491.
[88] I.A. Ribeiro, J. Rocha, B. Sepodes, H. Mota-Filipe, M.H. Ribeiro, Effect of naringin enzymatic hydrolysis towards naringenin on the anti-inflammatory activity of both compounds, J. Mol. Catal. B Enzym. 52–53 (2008) 13–18.
[89] L. Di Donna, G. Gallucci, N. Malaj, E. Romano, A. Tagarelli, G. Sindona, Recycling of industrial essential oil waste: Brutieridin and Melitidin, two anticholesterolaemic active principles from bergamot albedo, Food Chem. 125 (2011) 438–441.
[90] Y. Uesawa, K. Mohri, The use of heat treatment to eliminate drug interactions due to grapefruit juice, Biol. Pharm. Bull. 29 (2006) 2274–2278.